Effect of the polymer structure on the viscoelastic and interfacial healing behaviour of poly(urea-urethane) networks containing aromatic disulphides

Grande, A. M.; Martin, R.; Odriozola, I; van der Zwaag, S.; Garcia, S. J.

Important note
To cite this publication, please use the final published version (if applicable).
Please check the document version above.

Effect of the polymer structure on the viscoelastic and interfacial healing behaviour of poly(urea-urethane) networks containing aromatic disulphides

A.M. Grande[a], R. Martin[b], I. Odriozola[b], S. van der Zwaag[a], S.J. Garcia[a],*

[a] *Novel Aerospace Materials Group, Faculty of Aerospace Engineering, Delft University of Technology, Kluyverweg 1, 2629 HS Delft, The Netherlands*
[b] *Materials Division, IK4-CIDETEC Research Centre, Paseo Miramón 196, 20009 Donostia-San Sebastián, Spain*

ABSTRACT

The macroscopic interfacial healing behaviour in a series of urea-urethane networks as function of the hydrogen bonds and disulphides content is presented. The polymers were prepared with different crosslinking densities but with the same amount of dynamic covalent bonds (disulphide linkages). Tensile and fracture measurements were adopted to evaluate the degree of recovery of the mechanical properties after damage. Healing kinetics and healing efficiencies were quantitatively determined as a function of network composition, healing temperature and contact time. Finally, the recovery of mechanical properties was correlated with the viscoelastic response of the networks through rheological measurements and time-temperature superposition principle (TTS). The application of the TTS approach on both fracture healing and DMTA and subsequent mathematical descriptive model led to a better understanding of the influence of polymer architecture and that of the amount of reversible groups on the healing process.

1. Introduction

Intrinsic healing polymers have gained an increasing amount of attention in the last years due to their appealing ability to, autonomously or on-demand, repair (multiple times) mechanical damage, such as surface scratches and through-the-thickness cracks. A great challenge in the development of these new materials is to achieve a combination of a reasonable healing capability (i.e. more or less complete recovery of the base mechanical properties after a modest healing time in the range of 1–24 h at or close to the intended use temperature) and mechanical properties comparable to those of conventional non-self-healing polymer grades of the same polymer family. Significant efforts have been made by the polymer community to conceive and synthesize new polymeric materials with a high healing capability based on reversible non-covalent interactions or reversible covalent bonds [1–4]. Polymers based on reversible supramolecular interactions (e.g. multiple hydrogen bonding [5,6], van der Waals interactions by side branches [7] or metal-ligand coordination [8]) can show excellent healing at (near) room temperature and can have mechanical properties similar to those of conventional polymers when measured under short-term quasi-static loading conditions. However, due to the dynamic nature of the reversible bonds, these self-healing polymers have a significant temperature-dependent behaviour and a poor long-term mechanical stability. On the other hand, polymeric networks based on dynamic covalent

bonds (e.g. polysulphide [9–11], acylhydrazone bonds [12], boronic ester bonds [13] or Diels-Alder reaction [14]) potentially offer higher and more stable mechanical properties over a wider temperature range as a result of the higher stability of the reversible bond moiety. The unavoidable down side of this it that these polymers have a lower healing capacity at room temperature. A combination of both strategies might be a good approach to obtain better healing polymers with improved mechanical properties.

Already in 1963, Tobolsky demonstrated the significant effect of reversible polysulphide crosslinks on the viscoelastic behaviour of different polymers such polyethylene tetrasulphide [15] and urethane elastomers [16]. The unusual stress-relaxation behaviour of such polymers was attributed to a dynamic polysulphide bond interchange mechanism. Recently, different polysulphide based polymers exhibiting decent mechanical properties as well as an efficient healing performance have been developed [17]. Various triggering agents such as temperature [10,11,18], redox reactions [19] or UV-irradiation [20] can be used to induce selective scission of polysulphide bonds. The reshuffling rate of polysulphide can be accelerated by catalysts [21,22] and its temperature reduced when the appropriate monomers are selected as recently shown with aromatic disulphide based poly(urea-urethane) system (PUU) healing at room temperature in the absence of a specific catalyst [23]. This crosslinked PUU system containing disulphide bridges connected to aromatic groups can be reprocessed after

---

curing by applying high temperature and pressure in a mould, leading to products with a new shape without any loss in mechanical properties [24]. This system has been reported to be based on a unique combination of two self-healing mechanisms: H-bonds and aromatic disulphide metathesis. The latter mechanism is based on a [2 + 1] radical-mediated bonds exchange as reported somewhere else for disulphide containing polymers [25,26].

Despite the many attempts to develop new chemistries leading to strong and fast healing polymers, little attention has been yet placed on understanding the effect of the polymer architecture on healing even though polymer architecture is expected to have a major impact on kinetics and healing degree [27]. In the present work, we investigate the effect of the polymer structure on the healing behaviour of a series of PUU polymers with similar formulation and a fixed disulphide content but a variable crosslinking density. The testing framework includes a study of the main relaxation processes as detected by Dynamic Mechanical Thermal Analysis (DMTA) and a study of the recovery of the mechanical properties after cutting the samples at room temperature using dedicated tensile and fracture testing protocols. A Time Temperature Superposition protocol was applied to both the rheological and fracture results demonstrating a close relation between the main underlying processes responsible for macroscopic healing and polymer dynamics and the polymer architecture.

2. Experimental section

2.1. Materials

Poly(propylene glycol)s (PPG) of M_n = 6000 g mol^{-1} (PPG 6000, trifunctional) and M_n = 4000 g mol^{-1} (PPG 4000, linear difunctional) were purchased from Bayer Materials Science (Fig. 1). The M_n and M_w of PPGs were verified by size exclusion chromatography (SEC) and are provided in the Supporting Information. Isophorone diisocyanate (IPDI, 98%), dibutyltin dilaurate (DBTDL, 95%), bis(4-aminophenyl) disulphide (Linker) and tetrahydrofurane (THF) were purchased from Sigma-Aldrich and were used as received. The following synthesis steps were carried out in accordance with the procedure described by Rekondo et al. [23].

2.2. Synthesis of tris-isocyanate-terminated pre-polymer (PU 6000)

Mixtures of PPG (M_n = 6000 g mol^{-1}, 390 g, 65 mmol) and IPDI (45.45 g, 204.5 mmol) were fed into a 1 L glass reactor equipped with a mechanical stirrer and a vacuum inlet. The mixture was degassed by stirring under vacuum while heating to 70 °C for 10 min. Then, DBTDL (50 ppm) was added and the mixture was further stirred under vacuum at 70 °C for 45 min. The resulting tris-isocyanate terminated pre-polymer was obtained in the form of a colourless liquid and stored in a tightly closed glass bottle.

2.3. Synthesis of bis-isocyanate-terminated pre-polymer (PU 4000)

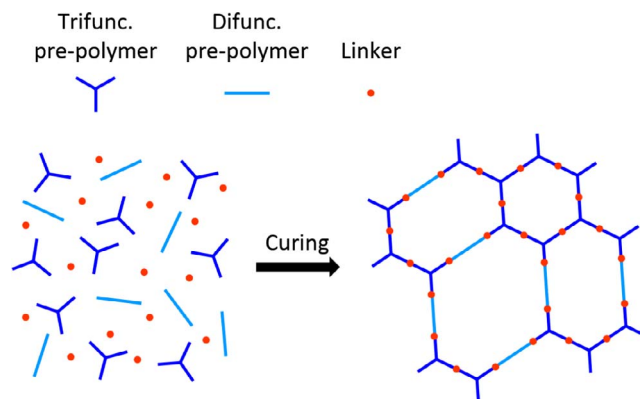A mixture of PPG (M_n = 4000 g mol^{-1}, 250 g, 62.5 mmol) and IPDI

Fig. 2. Chemical route followed in the preparation of the polymers under study.

(27.75 g, 125 mmol) were fed into a 1 L glass reactor equipped with mechanical stirrer and a vacuum inlet. The mixture was degassed by stirring under vacuum while heating at 60 °C for 10 min. Then DBTDL (50 ppm) was added and the mixture was further stirred under vacuum at 60 °C for 70 min.

2.4. Synthesis of self-healing poly(urea-urethane) networks with different crosslinking density (PUU systems)

The preparation of polymers containing the same quantity of disulphide moieties but different crosslinking densities was accomplished by using different combinations of the trifunctional polyurethane and difunctional polyurethane pre-polymers described above (PU 6000 and PU 4000). With this particular choice of precursors it was possible to keep the crosslinker quantity constant (1.2 eq. with respect to the NCO groups) as the equivalent weight of a chain between an isocyanate moiety and a crosslinking point is always 2000 g mol^{-1} (see Fig. 2). We varied the trifunctional:difunctional pre-polymer ratio from 100:0 to 70:30 (4 different ratios) as reported in Table 1. The stirred mixtures were poured in an open mould and cured for 16 h at 60 °C to produce approximately 2 mm thick films.

By introducing difunctional units, the number of bonds between the trifunctional units increased producing networks with lower crosslinking densities and thus an apparent higher molecular weight between the centres of the transiently connected three-arm molecules. The four polymers developed (Table 1) therefore contain the same density of disulphide and hydrogen bonds but differ in the crosslinking degree yet maintaining comparable glass transition temperatures (T_g). Such an approach allows for a dedicated study on the effect of the polymer architecture on healing.

2.5. Dynamic Mechanical Thermal Analysis (DMTA)

DMTA measurements were performed on a Thermo Scientific (model Haake™ Mars III) rheometer equipped with a temperature controlled test chamber and adopting the 20 mm parallel plate
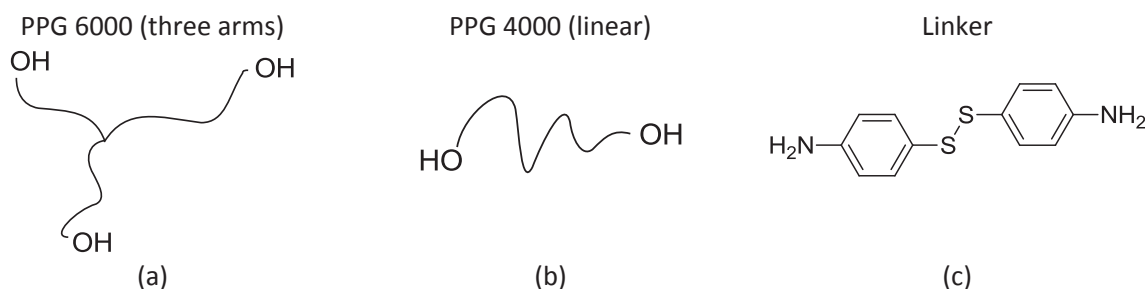

Fig. 1. Chemical sketch of PPGs (a-trifunctional, b-difunctional) and disulphide linker (c).

Table 1
Formulation and basic polymer properties of the studied systems.

Sample	Composition [wt%]			ν^a [mol/cm^3]	T_g^b [°C]
	PU-6000 (Trifun.)	PU-4000 (Difun.)	Linker		
PUU 100:0	93.8	0	6.2	$2.35 \cdot 10^{-4}$	−58.8
PUU 90:10	84.4	9.4	6.2	$2.05 \cdot 10^{-4}$	−59.0
PUU 80:20	75.1	18.7	6.2	$1.77 \cdot 10^{-4}$	−59.4
PUU 70:30	65.7	28.1	6.2	$1.50 \cdot 10^{-4}$	−60.1

[a] Theoretical crosslinking densities calculated from the nominal molecular weights between crosslinks; polymer density = 1 g/cm^3.

[b] T_g of the cured materials calculated from DSC experiments at 20 °C/min (see Supporting Information).

geometry. Frequency sweep experiments (0.01–10 Hz) were carried out in the small amplitude range (0.5% strain) at fixed temperatures ranging from 20 to 180 °C. Temperature steps of 20 °C were employed.

2.6. Tensile tests

Dumbbell-shaped specimens (ISO 527 A standard) were cut from the as-prepared 2 mm films in order to perform tensile strength measurements. Uniaxial tensile testing was conducted at crosshead speeds of 5, 50 and 500 mm/min corresponding to an estimated initial strain rate ($\dot{\epsilon}$) of $3 \cdot 10^{-3}$, $3 \cdot 10^{-2}$ and $3 \cdot 10^{-1} \, s^{-1}$, respectively. Some of the specimens were mechanically tested as virgin samples. The remaining samples were cut perpendicularly near the centre of the gauge length and then mended by bringing the two cut surfaces in (well aligned) contact and left to heal at room temperature (RT) for different periods of time (1, 6, 12 and 24 h) without any pressure applied. Typically, the time between cutting the samples with fresh razor blades and bringing the two cut surfaces back in contact was less than 3 min. The healed samples were tested immediately after the end of the healing period using the same testing protocol as for the pristine samples. At least 3 specimens per combination of polymer composition, healing time and strain rate were tested. Both the healing and the mechanical testing were done at room temperature.

2.7. Fracture tests

Single Edge Notch Tensile (SENT) specimens (70 × 20 mm) were obtained using a rectangular die and the moulded 2 mm flat polymeric sheets. A pre-notch with a length of approximately 10 mm was introduced in the samples using a sharp razor. SENT specimens were then clamped in the tensile machine and stretched until failure. A gauge length of 40 mm was employed in all fracture tests. Subsequently, fractured samples were accurately positioned in the original PTFE moulds and healed according to a previous published procedure [28,29]. The effects of both healing time and healing temperature on the recovery of fracture properties were investigated. Different samples were healed at various (constant) temperatures for 1, 3, 6 or 24 h; the healing temperature ranged from room temperature (RT ≈ 20 °C) to 120 °C. The healed samples were then re-tested after thermal equilibration at RT (about 30 min) following the original SENT fracture protocol. A constant crosshead speed of 60 mm/min (estimated initial strain rate $\dot{\epsilon} = 2.5 \cdot 10^{-2} \, s^{-1}$) was employed in each experiment and force and displacement data were collected. Video images were recorded during each experiment in order to detect crack initiation and to follow crack evolution. A typical sequence is shown in Fig. 3.

3. Results and discussion

3.1. Dynamics and mechanics of the polymeric networks

3.1.1. Viscoelastic response

From frequency sweep measurements, performed at different temperatures and applying the Time-Temperature Superposition (TTS) principle [30] the viscoelastic response of the different polymers were evaluated over a broad frequency range at the reference temperature of 20 °C. Storage modulus (G′), loss modulus (G″) and tan(δ) master curves were obtained. Although the validity of TTS for transient networks has been debated [31], TTS represents a useful method for a qualitatively evaluation of the dynamics of the relaxation processes occurring in this kind of polymeric networks [29,32–39].

The results for the various polymers are shown in Fig. 4. For all polymers two regimes in the analysed frequency range can be observed: (i) an elastic regime (G′ > G″) at high and moderate frequency and (ii) a viscous regime (G″ > G′) at low frequency. As can be observed from their tan(δ) master curves, the different regimes are characterized by a broad relaxation process spanning from 10 to about 10^{-5} rad/s and by a sharper one below $< 10^{-5}$ rad/s. These relaxation processes are also reflected in the G′ master curves of PUU 100:0, PUU 90:10 and PUU 80:20, where a change in slope can be detected below the threshold frequency (about 10^{-5} rad/s). The same slope change cannot be detected unambiguously for PUU 70:30.

As the content of difunctional moieties increases, a clear change in the variation of the elastic response of the PUU networks can be detected. The broad relaxation in the moderate frequency range leads to a G′ plateau region (corresponding to a local minimum in the tan(δ) around 10^{-5} rad/s). The G′ plateau value changes from about $6.5 \cdot 10^4$ Pa for PUU 100:0 to $2 \cdot 10^3$ Pa for PUU 70:30. This behaviour is in line with the calculated theoretical crosslinking densities. Furthermore, the tan(δ) values in the frequency range from 10 to 10^{-5} rad/s increase with increasing content of difunctional units, leading to a stronger viscoelastic response in PUU 70:30 than in PUU 100:0. The characteristic relaxation time τ_d ($\tau_d = 1/\omega_d$ where ω_d is the G′-G″ crossover frequency) associated with the terminal relaxation, decreases from about $5.3 \cdot 10^6$ s for PUU 100:0 to $7.2 \cdot 10^4$ s for PUU 70:30, suggesting an effect of the polymer structure on this relaxation process too.

Fig. 5 shows the temperature dependent shift factors (a_t) obtained from the master curve construction for the four polymers (Fig. 4). Interestingly, we observe similar a_t values and temperature dependences for all polymer grades. This suggests that the underlying transition processes controlling the t-T response in all the polymer grades is the same as suggested for other systems elsewhere [33].

When carefully looking at the curves in Fig. 4 at least two broad relaxations become apparent: one at high frequencies and one at low frequencies. Such multiple relaxation modes have previously been assigned to the plurality of the reversible moieties present in the polymeric networks [23,29]. The interchain H-bonds between urea groups are physical constraints and influence the movement of the chain branches formed from the connected arms of the trifunctional and difunctional units. Upon an external load, the natural fluctuations of the H-bonds allow the relaxation of the polymeric network by transverse chain motion (constraints release) [40]. The intensity of this relaxation is thereby related to the average molecular weight of the chain branches between the crosslinking points. Longer branches can afford larger movements leading to a stronger stress relaxation, as in the case of PUU 70:30. As the relaxation time or the temperature are increased, the reshuffling of the disulphide bonds facilitates the diffusion of the trifunctional and difunctional units through the network resulting in the loss of the elastic properties of the polymers and the complete release of the stress (viscous behaviour). The network structure embedding the dynamic covalent bonds affects the terminal relaxation process since smaller molecules can diffuse faster than larger one, as quantified in the

Fig. 3. Frames of video for fracture test on SENT specimens.
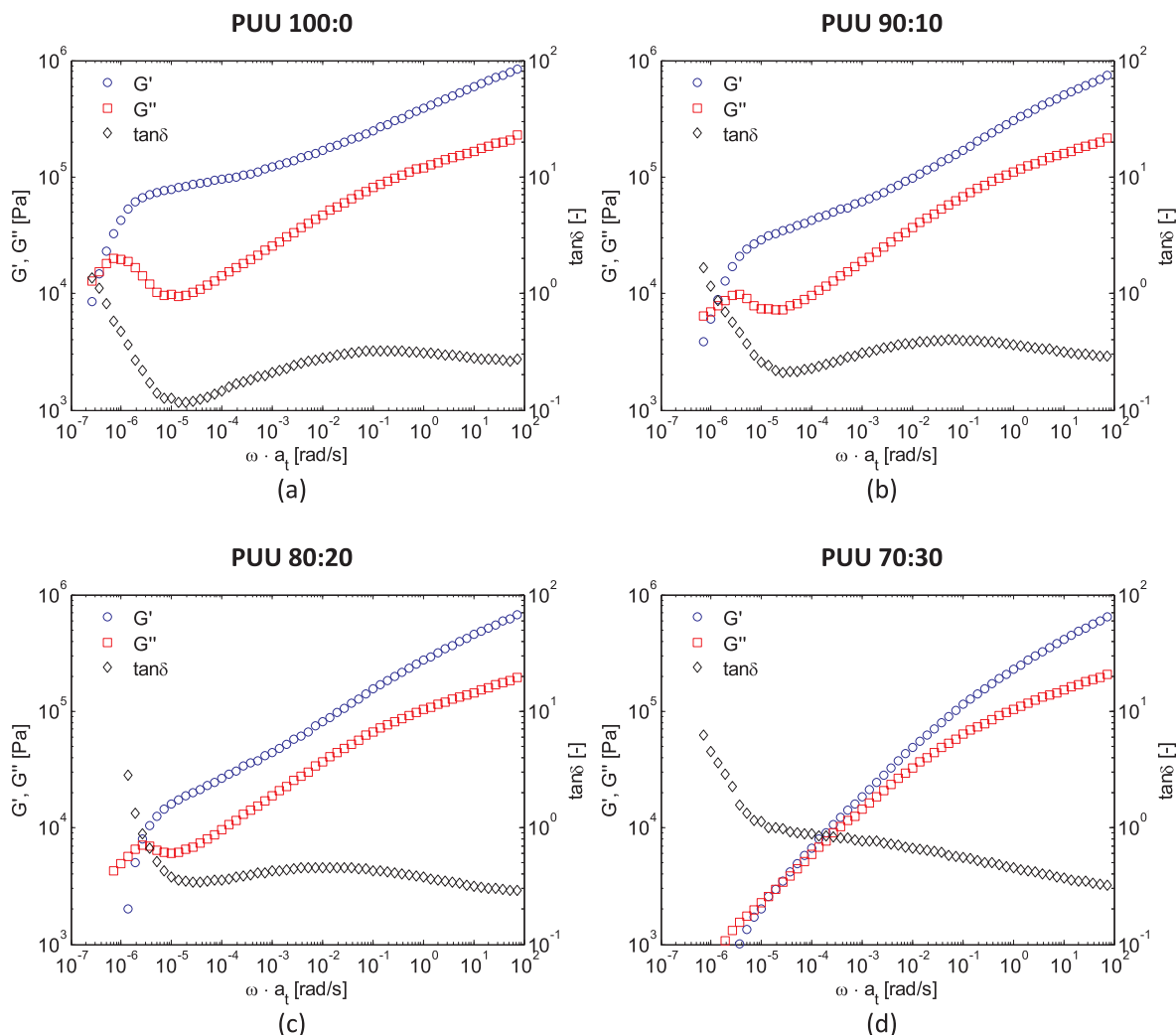
Fig. 4. Master curves (T_{ref} = 20 °C) for the different PUU grades.

Stokes-Einstein relation [41]. Thus, the networks with higher content of difunctional units should have a shorter characteristic relaxation time for the terminal relaxation.

Fig. 6 depicts the tensile stress-strain curves of the different polymers tested at various $\dot{\varepsilon}$. The polymers exhibit a classical rubber-like behaviour characterized by an initial elastic region, a high elongation and some strain hardening. As predicted by the DMTA analysis, a strong viscoelastic response at RT can also be observed: all polymer grades have strain-rate dependent tensile properties. Tensile data are summarized in Table S1 (see Supporting Information). Polymers with lower di-functional unit content show a higher initial tensile modulus (E), a higher stress at break (σ_b) and a lower strain at break (ε_b) irrespective of the $\dot{\varepsilon}$. As in standard polymers, these trends can be related to the

different crosslinking density in the polymeric networks. Secondly, an increase in E, σ_b and ε_b with increasing $\dot{\varepsilon}$ is detected for all polymer grades. At higher $\dot{\varepsilon}$, the weak physical bonds (H-bonds) can act as quasi-permanent links causing the measured increase in strength and modulus.

In order to assess the contribution of the elastic and viscous response to the global tensile behaviour the obtained experimental results were fitted to mathematical models. Interestingly, it was not possible to accurately describe the tensile behaviour of the tested PUU systems by means of hyperelastic models [42] commonly used for rubber-like materials based on crosslinked non-reversible networks. A refined viscoelastic model being a combination of the Upper Convected Maxwell (UCM) model [43] and the Gent strain hardening model (Gent) [44]
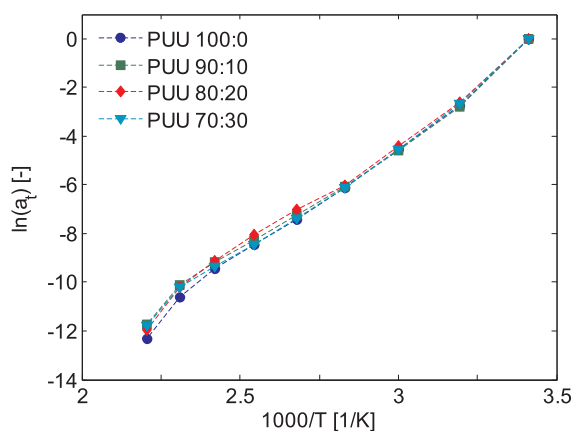
Fig. 5. Shift factors (a$_t$) obtained from the master curves construction for the different polymer grades (reference temperature of 20 °C).

was used instead (see Supporting Information, Fig. S7). This model, originally developed to describe the mechanical response of soft-soft nanocomposites [45], has been reported to accurately capture the tensile behaviour of hybrid polymers and physical hydrogels [46,47]. From the values of the model parameters G$_e$, G$_v$ (Supporting Information, Table S2), it was possible to identify the elastic response related to irreversible and temporary strong bonds (G$_e$), the viscous response here attributed to the weak transient bonds in the polymer network (G$_v$) and the extensibility of the network (J$_m$). Furthermore, as reported elsewhere [47] it was possible to relate the ratio G$_v$/G$_e$ to the ratio of polymer chains constrained by weak interactions and permanent ones. The evolution of the extracted characteristic parameters G$_e$ and G$_v$ as a function of the difunctional units content is plotted in Fig. 7. At the highest strain rate ($\dot{\varepsilon} = 3 \cdot 10^{-1}\,s^{-1}$), for all the polymer grades, a nearly constant G$_v$ value can be observed; on the other hand, G$_e$ decreases with the increase of difunctional units, in line with PUU 100:0 having a higher theoretical crosslinking density than PUU 70:0. The resulting G$_v$/G$_e$ increases from 1 for the network without difunctional units to about 2 for PUU 70:30 (30% difunctional units content). These results confirm that more weak constraints between two connected trifunctional units are present in PUU 70:30 than in PUU 100:0.

The results of the fitting of experimental tensile data reflect the viscoelastic behaviour of the networks observed in the DMTA analyse. Both G$_e$ and G$_v$ decrease with the decrease of $\dot{\varepsilon}$ for all the polymer grades, indicating that the contributions of weaker temporary bonds effectively disappear a low strain rates and that the present weak bonds have a minor role on the networks strength at low strain rates. This effect is more evident for PUU 70:30 (greater decrement of G$_v$/G$_e$ from high to low $\dot{\varepsilon}$), highlighting its stronger viscoelastic response compared to networks containing a lower amount of difunctional units.

Further insight in the tensile response of the network can be obtained by analysing the strain rate dependent evolution of the J$_m$ (Table S2, Supporting Information), parameter which reflects the assumed finite extensibility of the network. J$_m$ significantly varies with strain rate from a relative low value at a high deformation rate to a value over 10,000 at a low deformation rate, irrespective of the polymer type. This latter value is in line with that of poorly crosslinked polymeric networks [45], indicating a change in the networks connectivity during slow stretching at large deformation.

While the effect of the weak H-bonds on the global tensile response at large deformation is limited, intrachain disulphide bonds play a crucial role on the elastic response of the material being responsible of the connection between adjacent polymer chains. However, in case of a large deformation (high chain stress) and a slow strain rate, the disulphide bonds can break and potentially reform with enhanced kinetics [48]; under these testing conditions the characteristic total exchange time of the dynamic covalent bonds increases resulting in the same
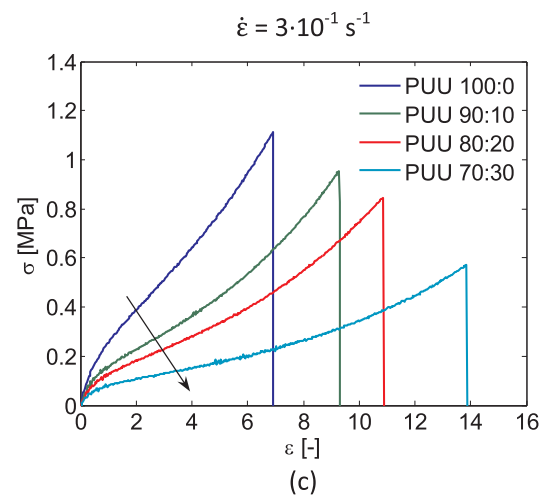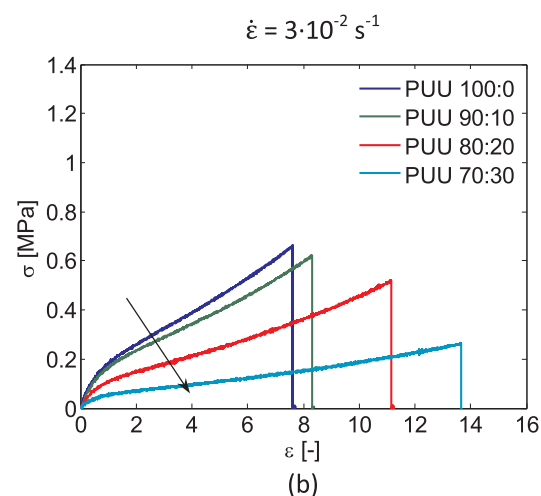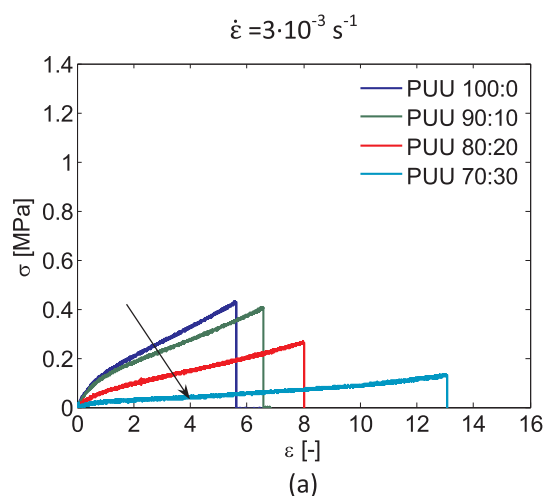

(a)

(b)

(c)

Fig. 6. Stress-strain curves for PUU networks tested at the nominal strain rate of $3 \cdot 10^{-3}\,s^{-1}$ (a), $3 \cdot 10^{-2}\,s^{-1}$ (b) and $3 \cdot 10^{-1}\,s^{-1}$ (c). Arrows in the plots indicate the increment in difunctional units content.

order magnitude of the rate at which the polymeric network is stretched. This explains the change in network connectivity described by the variation of parameter J$_m$.

3.1.2. Fracture mechanics
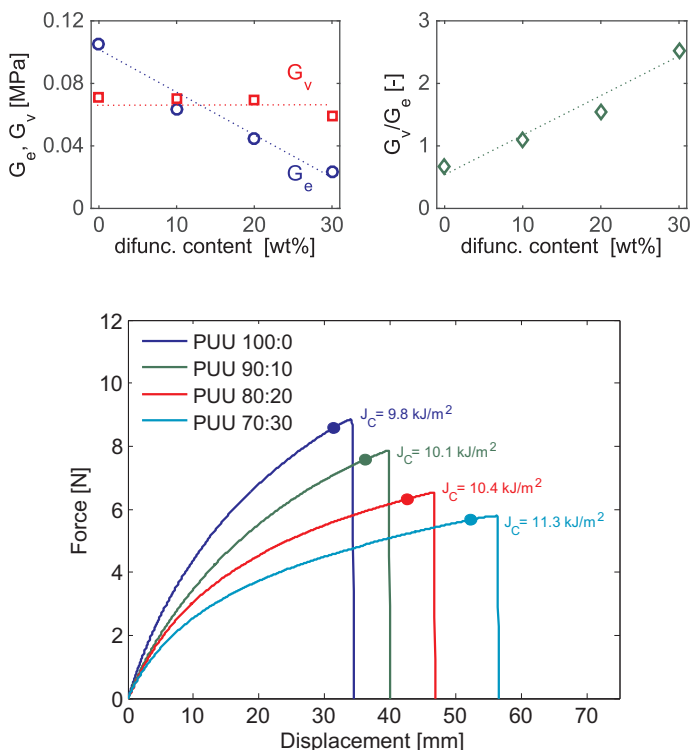Fracture mechanics tests provide a different perspective on the

Fig. 8. Load-Displacement curves and calculated J_C values for the different polymer grades. The markers indicate the crack initiation, as detected by video analysis.
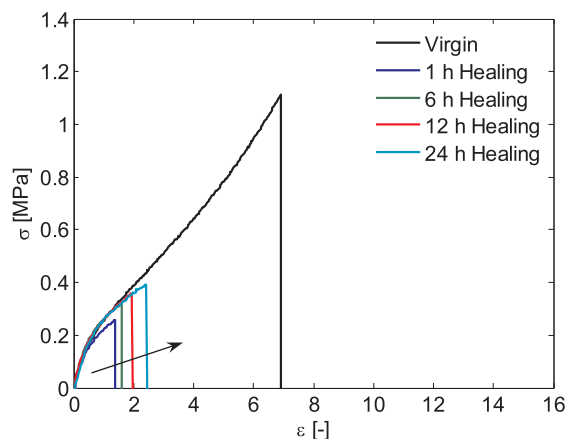

Fig. 9. Stress-Strain curves for virgin and healed PUU 100:0 samples tested in tensile mode at $\dot{\varepsilon} = 3 \cdot 10^{-1} \, \text{s}^{-1}$. The arrow in the plot indicates the increment in healing time.

mechanical performance of a material. Unlike tensile experiments, where the sample is loaded with a quasi-homogeneous stress distribution, in fracture experiment, the notched sample geometry ensures stress localization at the crack tip zone. Typical Load-Displacement curves for the tested SENT geometry are shown in Fig. 8. From these curves, fracture properties can be determined by J-integral approach [28,49]. Critical fracture energy values, J_c, for each sample were calculated according to the following equation:

$$J_c \, [\text{kJ/m}^2] = \left. \frac{\eta U_c}{b(w-a)} \right|_{u_c} \tag{1}$$

where U_c is the energy calculated as the area under the Load-Displacement curves at the displacement u_c where crack propagation occurs, η. the proportionality factor (a value of 0.9 was selected according to literature [49]); b, w and a are the sample thickness, sample width and pre-crack length, respectively.

As in tensile tests, lower stress and higher stretch levels are detected for the polymers containing higher amounts of difunctional units. A higher value of J_c indicates that during fracture testing more energy is dissipated by the network.

3.2. Healing behaviour after damage

3.2.1. Recovery of tensile properties

The stress at break (σ_b) is considered as the reference value for the evaluation of the healing ability in tensile mode. The tensile healing efficiency of each composition is determined as the relation between the stress at break of the healed samples (σ_b^{healed}) and that of the virgin samples (σ_b^{virgin}) for a specific healing time and a specific $\dot{\varepsilon}$:

$$\textit{Tensile Healing efficiency} \, [\%] = \frac{\sigma_b^{healed}}{\sigma_b^{virgin}} \cdot 100 \tag{2}$$

Fig. 9 shows an example of the influence of healing time on the stress-strain behaviour of PUU 100:0. The tensile healing efficiency values at $\dot{\varepsilon} = 3 \cdot 10^{-1} \, \text{s}^{-1}$, as calculated using Eq. (2), for different

healing time are reported for all materials in Fig. 10(a). The different polymers show different tensile healing efficiency as a function of healing time. Polymer grades with a higher difunctional unit content showed a greater healing efficiency at any given time.

As shown in Fig. 10(b), the applied strain rate has significant effect on the measured healing efficiency. All polymer grades show a marked reduction in the recovered stress at break if tested at low strain rates. The highest decrement is detected for PUU 70:30 from about 80% at $\dot{\varepsilon} = 3 \cdot 10^{-1} \, \text{s}^{-1}$ to about 30% at $\dot{\varepsilon} = 3 \cdot 10^{-3} \, \text{s}^{-1}$ for 24 h healing at RT. These results are in good agreement with those we previously reported for a H-bonds containing elastomer [28].

3.2.2. Recovery of fracture properties

The recovery in interfacial properties for the PUU networks was evaluated following the same damage and J-integral fracture mechanics protocol developed and used in previous studies on self-healing elastomers [28,29]. The healing time and healing temperature were varied over the range 1–24 h and from RT to 120 °C, respectively. Representative Load-Displacement curves obtained for PUU 70:30 SENT samples healed for different times and at different temperatures are shown in Fig. 11. At room temperature the system shows a limited recovery of the initial fracture properties even after healing for 24 h (Fig. 11(a)). The material shows instead a clear temperature dependent recovery of fracture energy with increasing healing temperature (Fig. 11(b)). Similar results were obtained for the other compositions.

To quantify the recovery of fracture properties [28,29], J_C is selected as reference parameter and the healing efficiency in fracture mode is calculated as the ratio between the measured J-integral for healed (J_C^{healed}) and virgin samples J_C^{virgin}:

$$\textit{Fracture Healing efficiency} \, [\%] = \frac{J_C^{healed}}{J_C^{virgin}} \cdot 100 \tag{3}$$

Fracture healing efficiency values as a function of healing time and temperature are presented in Fig. 12(a) for PUU 70:30. At RT, a maximum fracture healing efficiency of about 20% after 24 h is obtained. A higher healing temperature significantly increased the healing
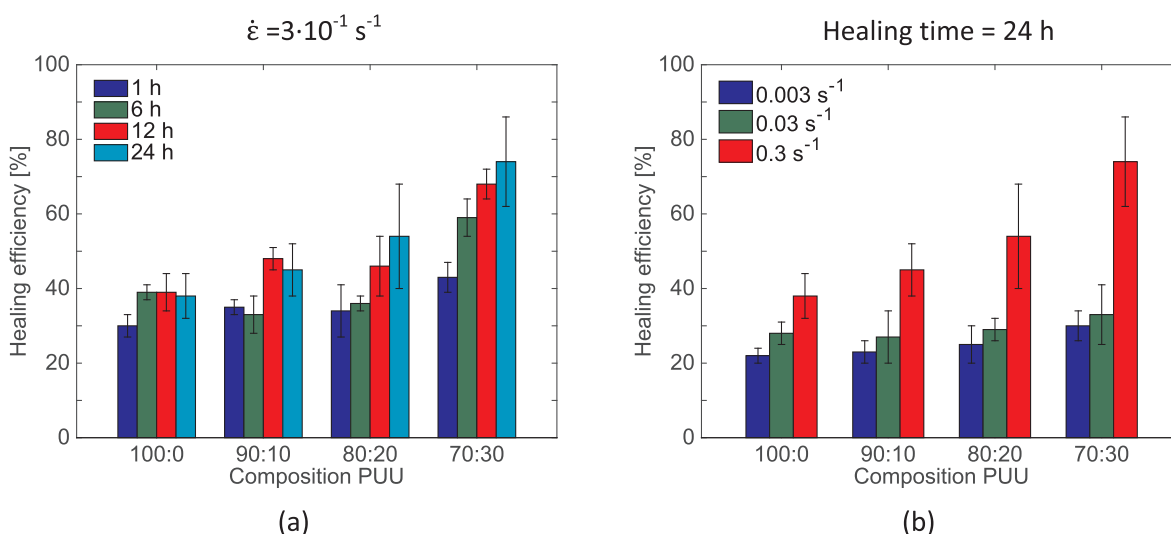
Fig. 10. Healing efficiency values for different healing time at constant strain rate (a) and for different strain rate at constrain healing time (24 h).

efficiency resulting in an almost complete recovery of the original fracture energy after a 6 h healing treatment at 120 °C.

The other polymer grades recovered their fracture energy values to a comparable but always lower healing efficiency than PUU 70:30 (see Supporting information, Fig. S4), in agreement with tensile tests. Both in tensile and fracture mode, the healing efficiency is improved when the molecular weight between crosslinking points is high (low crosslinking density), which affects the length of the resulting dangling chains at the damaged interface [50]. However, after healing at RT and relative short healing time (< 24 h), none of the tested polymers exhibit a complete recovery of the original mechanical (tensile and fracture) properties. A possible explanation can be given by considering that reversible covalent bonds are not reformed and only weak bonds and diffused chains are present in the healed region. Although disulphide groups can exchange sulphur bonds around room temperature [23,51], the kinetics of the radical-mediated reshuffling of these bonds is too slow for an efficient recovery of the interfacial properties in all the polymer grades, as demonstrate by low strain rate tensile and fracture tests on lower temperature healed samples. High strain rate tensile experiments on healed samples do not provide a complete and clear view on the recovered interfacial properties. It follows that higher temperatures and/or longer healing times are necessary to activate/promote an efficient reformation of the reversible covalent bonds and thus a (almost) complete recovery of the original mechanical

properties.

As recently demonstrated [29,39,52], it is possible to build a fracture-healing master curve at a reference temperature by shifting along the x-axis the healing efficiency values obtained at different temperatures, in analogy with viscoelastic master curve construction. This procedure allows investigating the healing performance of healable systems over a broad time range, as shown in Fig. 12(b). Furthermore, the correspondence of the shift factors from healing and rheological master curves (inset in Fig. 12(b)) demonstrates that both phenomena are governed by the same mechanisms as previously observed in other healing polymers [29].

The fracture-healing master curves for each composition are plotted in Fig. 13. A higher degree of healing in a shorter time is detected for those grades with the higher difunctional pre-polymer content (e.g. PUU 70:30 vs PUU 100:0). In agreement with our previous work on a comparable system [29] we assign the initial healing at short times to short range interactions [7] and diffusion related to H-bonding [28]. This process seems to be in this case accelerated with lower crosslinking densities (higher slopes). The second process initiates at longer healing times but then has a larger contribution to the overall recovery of the mechanical interfacial properties and this is attributed to the reformation of disulphide bonds. It should be noted that even if this second process initiates at different times depending on the crosslinking density it keeps the same kinetics for the four compositions; this indicates

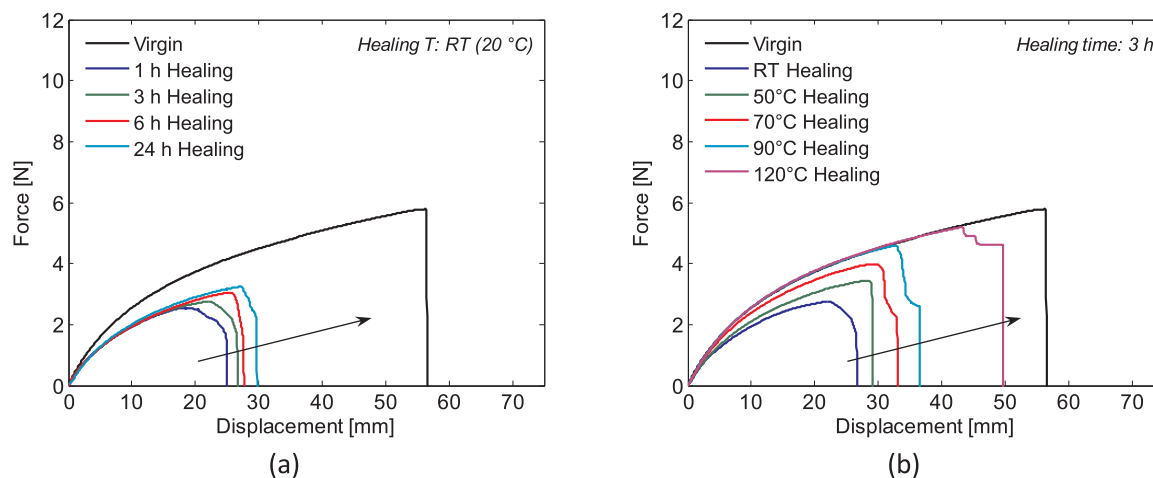**Fig. 11.** Load-Displacement curves obtained in fracture mode for healed PUU 70:30 samples. Effect of healing time (a) and healing temperature (b). Arrows in the plots indicate the increment in healing time and healing temperature, respectively.
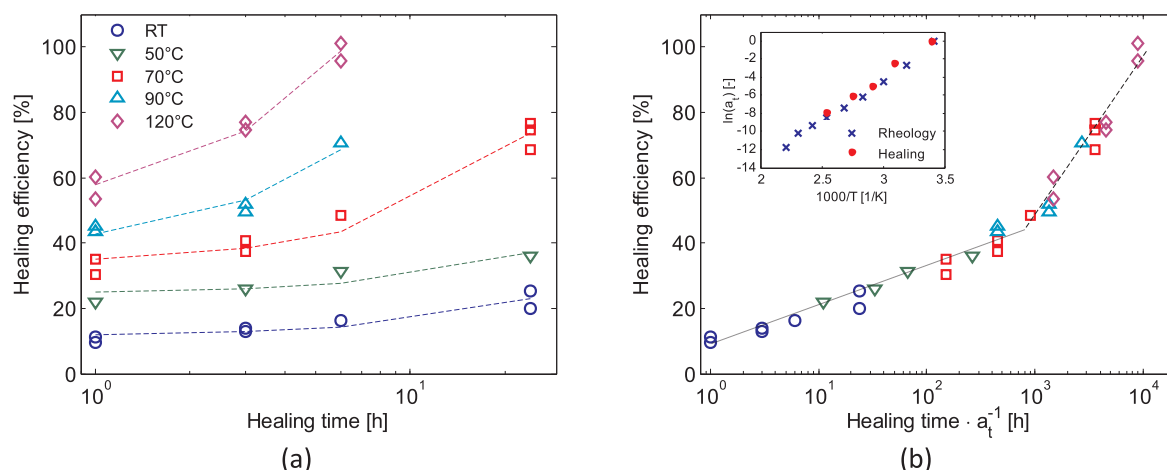
Fig. 12. Healing efficiency values for PUU 70:30 obtained from fracture experiments after healing at different temperature (a); dashed lines are as guides for the eye. Respective healing master curve (b) at the reference temperature of 20 °C; the inset shows shift factors (a_t) arising from rheological and healing master curves construction for PUU 70:30.
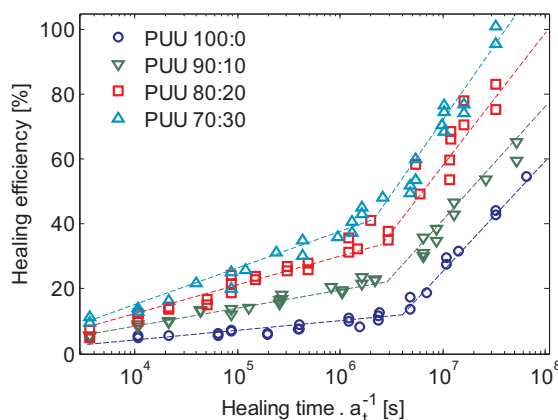

Fig. 13. Fracture healing efficiency master curves at the reference temperature of 20 °C. Dashed lines represent power laws used as guides for the eye.

the second relaxation is less affected by the crosslinking density than the fast initial recovery attributed to the H-bonding. This can be explained by the virtual breaking of the crosslinked network at long relaxation times.

By analysing the rheological and fracture healing master curves, it is clear that the two observed relaxation and healing steps might be potentially related. The compositional evolution of first healing stage, detected at lower healing time, follows the same trend of the broad relaxation observed at intermediate frequency range. As general rule, higher difunctional unit content promotes higher network mobility, greater viscoelastic and greater (limited) healing response. The second healing stage, occurring for all the polymer grades over the same healing time range (onset in Fig. 13), can be related to the second sharp relaxation characterized by a viscous behaviour of the networks due to the rearrangement of the reversible intramolecular dynamic covalent bonds (disulphide bonds). This viscous behaviour is a necessary condition for a full recovery of the initial network organization at the healed interfaces and original mechanical properties.

4. Conclusions

The healing ability of covalent reversible networks containing disulphides has been explored by tuning the structure of poly(urea-urethane) networks. The variation of polymer composition by the introduction of bis-isocyanate-terminated units (difunctional units) produced polymeric networks with different cross-link density but same amount of reversible covalent bonds.

This change in the network structure directly affects the mechanical properties as well as the healing response after damage. As a result, the polymers synthesized with high contents of difunctional units possess both high viscoelastic and healing properties, but low tensile strength. The insight into the role of the polymer structure on the healing process will benefit the design of new self-healing polymers with tailored mechanical properties.

Appendix A. Supplementary material

Supplementary data associated with this article can be found, in the online version, at http://dx.doi.org/10.1016/j.eurpolymj.2017.10.007.

References

[1] M.D. Hager, P. Greil, C. Leyens, S. Van Der Zwaag, U.S. Schubert, Self-healing materials, Adv. Mater. 22 (47) (2010) 5424–5430.
[2] F. Herbst, D. Döhler, P. Michael, W.H. Binder, Self-healing polymers via supramolecular forces, Macromol. Rapid Commun. 34 (3) (2013) 203–220.
[3] B. Sandmann, S. Bode, M. Hager, U. Schubert, Metallopolymers as an emerging class of self-healing materials, in: V. Percec (Ed.), Hierarchical Macromolecular Structures: 60 Years after the Staudinger Nobel Prize II: Springer International Publishing, 2013, pp. 239–257.
[4] L.M. de Espinosa, G.L. Fiore, C. Weder, E. Johan Foster, Y.C. Simon, Healable supramolecular polymer solids, Prog. Polym. Sci. 49–50 (2015) 60–78.
[5] R.P. Sijbesma, F.H. Beijer, L. Brunsveld, B.J.B. Folmer, J.H.K.K. Hirschberg, R.F.M. Lange, et al., Reversible polymers formed from self-complementary monomers using quadruple hydrogen bonding, Science 278 (5343) (1997) 1601–1604.
[6] P. Cordier, F. Tournilhac, C. Soulié-Ziakovic, L. Leibler, Self-healing and thermoreversible rubber from supramolecular assembly, Nature 451 (7181) (2008) 977–980.
[7] A. Susa, R.K. Bose, A.M. Grande, S. van der Zwaag, S.J. Garcia, Effect of the dianhydride/branched diamine ratio on the architecture and room temperature healing behavior of polyetherimides, ACS Appl. Mater. Interfaces 8 (49) (2016) 34068–34079.
[8] S. Bode, L. Zedler, F.H. Schacher, B. Dietzek, M. Schmitt, J. Popp, et al., Self-healing polymer coatings based on crosslinked metallosupramolecular copolymers, Adv Mater. 25 (11) (2013) 1634–1638.
[9] J.A. Yoon, J. Kamada, K. Koynov, J. Mohin, R. Nicolaÿ, Y. Zhang, et al., Self-healing polymer films based on thiol-disulfide exchange reactions and self-healing kinetics measured using atomic force microscopy, Macromolecules 45 (1) (2012) 142–149.
[10] U. Lafont, C. Moreno-Belle, H. Van Zeijl, S. Van Der Zwaag, Self-healing thermal conductive composites, 2012, pp. 1324–1329.
[11] M. AbdolahZadeh, C. Esteves AC, van der Zwaag S, Garcia SJ. Healable dual organic–inorganic crosslinked sol–gel based polymers: crosslinking density and tetrasulfide content effect, J. Polym. Sci., Part A: Polym. Chem. 52 (14) (2014) 1953–1961**.

[12] G. Deng, C. Tang, F. Li, H. Jiang, Y. Chen, Covalent cross-linked polymer gels with reversible sol−gel transition and self-healing properties, Macromolecules 43 (3) (2010) 1191–1194.

[13] O.R. Cromwell, J. Chung, Z. Guan, Malleable and self-healing covalent polymer networks through tunable dynamic boronic ester bonds, J. Am. Chem. Soc. 137 (20) (2015) 6492–6495.

[14] C. Toncelli, D.C. De Reus, F. Picchioni, A.A. Broekhuis, Properties of reversible diels-alder furan/maleimide polymer networks as function of crosslink density, Macromol Chem Phys. 213 (2) (2012) 157–165.

[15] A.V. Tobolsky, R.B. Beevers, G.D.T. Owen, The viscoelastic properties of crosslinked poly(ethylene tetrasulfide), I. J. Colloid Sci. 18 (4) (1963) 353–358.

[16] G.D.T. Owen, W.J. MacKnight, A.V. Tobolsky, Urethane elastomers containing disulfide and tetrasulfide linkages, J. Phys. Chem. 68 (4) (1964) 784–786.

[17] E.-K. Bang, M. Lista, G. Sforazzini, N. Sakai, S. Matile, Poly(disulfide)s, Chem. Sci. 3 (6) (2012) 1752–1763.

[18] J. Canadell, H. Goossens, B. Klumperman, Self-healing materials based on disulfide links, Macromolecules 44 (8) (2011) 2536–2541.

[19] J. Kamada, K. Koynov, C. Corten, A. Juhari, J.A. Yoon, M.W. Urban, et al., Redox responsive behavior of thiol/disulfide-functionalized star polymers synthesized via atom transfer radical polymerization, Macromolecules 43 (9) (2010) 4133–4139.

[20] H. Otsuka, S. Nagano, Y. Kobashi, T. Maeda, A. Takahara, A dynamic covalent polymer driven by disulfide metathesis under photoirradiation, Chem. Commun. 46 (7) (2010) 1150–1152.

[21] R. Caraballo, M. Rahm, P. Vongvilai, T. Brinck, O. Ramstrom, Phosphine-catalyzed disulfide metathesis, Chem. Commun. 48 (2008) 6603–6605.

[22] T. Oku, Y. Furusho, T. Takata, A concept for recyclable cross-linked polymers: topologically networked polyrotaxane capable of undergoing reversible assembly and disassembly, Angew. Chem. Int. Ed. 43 (8) (2004) 966–969.

[23] A. Rekondo, R. Martin, A. Ruiz de Luzuriaga, G. Cabanero, H.J. Grande, I. Odriozola, Catalyst-free room-temperature self-healing elastomers based on aromatic disulfide metathesis, Mater. Horiz. 1 (2) (2014) 237–240.

[24] R. Martin, A. Rekondo, A. Ruiz De Luzuriaga, G. Cabañero, H.J. Grande, I. Odriozola, The processability of a poly(urea-urethane) elastomer reversibly crosslinked with aromatic disulfide bridges, J. Mater. Chem. A 2 (16) (2014) 5710–5715.

[25] J.M. Matxain, J.M. Asua, F. Ruiperez, Design of new disulfide-based organic compounds for the improvement of self-healing materials, Phys. Chem. Chem. Phys. 18 (3) (2016) 1758–1770.

[26] M. Hernández, A.M. Grande, W. Dierkes, J. Bijleveld, S. van der Zwaag, S.J. García, Turning vulcanized natural rubber into a self-healing polymer: effect of the disulfide/polysulfide ratio, ACS Sustain. Chem. Eng. 4 (10) (2016) 5776–5784.

[27] S.J. Garcia, Effect of polymer architecture on the intrinsic self-healing character of polymers, Eur. Polym. J. 53 (1) (2014) 118–125.

[28] A.M. Grande, S.J. Garcia, S. van der Zwaag, On the interfacial healing of a supramolecular elastomer, Polymer 56 (2015) 435–442.

[29] A.M. Grande, J.C. Bijleveld, S.J. Garcia, S. van der Zwaag, A combined fracture mechanical – rheological study to separate the contributions of hydrogen bonds and disulphide linkages to the healing of poly(urea-urethane) networks, Polymer 96 (2016) 26–34.

[30] J.D. Ferry, Viscoelastic Properties of Polymers, Wiley, 1961.

[31] S. Seiffert, J. Sprakel, Physical chemistry of supramolecular polymer networks, Chem. Soc. Rev. 41 (2) (2012) 909–930.

[32] R.F.M. Lange, M. Van Gurp, E.W. Meijer, Hydrogen-bonded supramolecular polymer networks, J. Polym. Sci., Part A: Polym. Chem. 37 (19) (1999) 3657–3670.

[33] F.J. Stadler, W. Pyckhout-Hintzen, J.-M. Schumers, C.-A. Fustin, J.-F. Gohy, C. Bailly, Linear viscoelastic rheology of moderately entangled telechelic polybutadiene temporary networks, Macromolecules 42 (16) (2009) 6181–6192.

[34] J.R. Kumpfer, J.J. Wie, J.P. Swanson, F.L. Beyer, M.E. Mackay, S.J. Rowan, Influence of metal ion and polymer core on the melt rheology of metallosupramolecular films, Macromolecules 45 (1) (2012) 473–480.

[35] F. Herbst, S. Seiffert, W.H. Binder, Dynamic supramolecular poly(isobutylene)s for self-healing materials, Polym. Chem. 3 (11) (2012) 3084–3092.

[36] A. Shabbir, H. Goldansaz, O. Hassager, E. van Ruymbeke, N.J. Alvarez, Effect of hydrogen bonding on linear and nonlinear rheology of entangled polymer melts, Macromolecules 48 (16) (2015) 5988–5996.

[37] L.G.D. Hawke, M. Ahmadi, H. Goldansaz, E. van Ruymbeke, Viscoelastic properties of linear associating poly(n-butyl acrylate) chains, J. Rheol. 60 (2) (2016) 297–310.

[38] M. Abdolah Zadeh, A.M. Grande, S. van der Zwaag, S.J. Garcia, Effect of curing on the mechanical and healing behaviour of a hybrid dual network: a time resolved evaluation, RSC Adv. 6 (94) (2016) 91806–91814.

[39] R.K. Bose, M. Enke, A.M. Grande, S. Zechel, F.H. Schacher, M.D. Hager, et al., Contributions of hard and soft blocks in the self-healing of metal-ligand-containing block copolymers, Eur. Polym. J. 93 (2017) 417–427.

[40] L.L. De Lucca Freitas, R. Stadler, Thermoplastic elastomers by hydrogen bonding. 3. Interrelations between molecular parameters and rheological properties, Macromolecules 20 (10) (1987) 2478–2485.

[41] J.T. Edward, Molecular volumes and the Stokes-Einstein equation, J. Chem. Educ. 47 (4) (1970) 261.

[42] G. Marckmann, E. Verron, Comparison of hyperelastic models for rubber-like materials, Rubber Chem. Technol. 79 (5) (2006) 835–858.

[43] R.B. Bird, R.C. Armstrong, O. Hassager, Dynamics of Polymeric Liquids: Vol. 1 Fluid Mechanics, 2nd ed., Wiley, New York, 1987.

[44] A.N. Gent, A new constitutive relation for rubber, Rubber Chem. Technol. 69 (1) (1996) 59–61.

[45] F. Deplace, M.A. Rabjohns, T. Yamaguchi, A.B. Foster, C. Carelli, C.-H. Lei, et al., Deformation and adhesion of a periodic soft-soft nanocomposite designed with structured polymer colloid particles, Soft Matter 5 (7) (2009) 1440–1447.

[46] T. Wang, C. de las Heras Alarcón, M. Goikoetxea, I. Beristain, M. Paulis, M.J. Barandiaran, et al., Cross-Linked Network Development in Compatibilized Alkyd/Acrylic Hybrid Latex Films for the Creation of Hard Coatings, Langmuir, 2010, pp. 14323–14333.

[47] T.L. Sun, F. Luo, T. Kurokawa, S.N. Karobi, T. Nakajima, J.P. Gong, Molecular structure of self-healing polyampholyte hydrogels analyzed from tensile behaviors, Soft Matter 11 (48) (2015) 9355–9366.

[48] A.P. Wiita, S.R.K. Ainavarapu, H.H. Huang, J.M. Fernandez, Force-dependent chemical kinetics of disulfide bond reduction observed with single-molecule techniques, Proc. Natl. Acad. Sci. 103 (19) (2006) 7222–7227.

[49] G. Ramorino, S. Agnelli, R. De Santis, T. Riccò, Investigation of fracture resistance of natural rubber/clay nanocomposites by J-testing, Eng. Fract. Mech. 77 (10) (2010) 1527–1536.

[50] M. Yamaguchi, R. Maeda, R. Kobayashi, T. Wada, S. Ono, S. Nobukawa, Autonomic healing and welding by interdiffusion of dangling chains in a weak gel, Polym. Int. 61 (1) (2012) 9–16.

[51] S. Nevejans, N. Ballard, J.I. Miranda, B. Reck, J.M. Asua, The underlying mechanisms for self-healing of poly(disulfide)s, Phys. Chem. Chem. Phys. (2016).

[52] C.N.Z. Schmitt, Y. Politi, A. Reinecke, M.J. Harrington, Role of sacrificial protein-metal bond exchange in mussel byssal thread self-healing, Biomacromolecules 16 (9) (2015) 2852–2861.